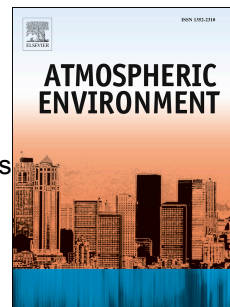# Accepted Manuscript

Spatio-temporal variations and influencing factors of polycyclic aromatic hydrocarbons in atmospheric bulk deposition along a plain-mountain transect in western China

Xinli Xing, Yuan Zhang, Dan Yang, Jiaquan Zhang, Wei Chen, Chenxi Wu, Hongxia Liu, Shihua Qi

Please cite this article as: Xing, X., Zhang, Y., Yang, D., Zhang, J., Chen, W., Wu, C., Liu, H., Qi, S., Spatio-temporal variations and influencing factors of polycyclic aromatic hydrocarbons in atmospheric bulk deposition along a plain-mountain transect in western China, *Atmospheric Environment* (2016), doi: 10.1016/j.atmosenv.2016.05.027.

Spatio-temporal variations and influencing factors of Polycyclic Aromatic Hydrocarbons in atmospheric bulk deposition along a plain-mountain transect in Western China

Xinli Xing[a, b], Yuan Zhang[b], Dan Yang[c], Jiaquan Zhang[d,e], Wei Chen[e], Chenxi Wu[f], Hongxia Liu[d], Shihua Qi[a, b*]

a School of Environmental studies, China University of Geosciences, Wuhan, 430074, China

b State Key Laboratory of Biogeology and Environmental Geology, China University of Geosciences, Wuhan, 430074, China

c Faculty of Engineering, China University of Geosciences, Wuhan 430074, China

d School of Environmental Science and Engineering, Hubei Polytechnic University, Huangshi 435003, China

e Lancaster Environmental Centre, Lancaster University, LA1 4YY, UK

f State Key Laboratory of Freshwater Ecology and Biotechnology, Institute of Hydrobiology, Chinese Academy of Sciences, Wuhan, 430072, China

ABSTRACT

Ten atmospheric bulk deposition (the sum of wet and dry deposition) samplers for polycyclic aromatic hydrocarbons (PAHs) were deployed at a plain-mountain transect (namely PMT transect, from Daying to Qingping) in Chengdu Plain, West China from June 2007 to June 2008 in four consecutive seasons (about every three months). The bulk deposition fluxes of $\sum_{15}$-PAHs ranged from 169.19 $\mu g\ m^{-2}\ yr^{-1}$ to 978.58 $\mu g\ m^{-2}\ yr^{-1}$ with geometric mean of 354.22 $\mu g\ m^{-2}\ yr^{-1}$. The most prevalent PAHs were 4-ring (39.65%) and 3-ring (35.56%) PAHs. The flux values were comparable to those in rural areas. Higher fluxes of total PAHs were observed in the middle of PMT transect (SL, YX and JY, which were more urbanized than other sites). The seasonal deposition fluxes in the sampling profile indicated seasonality of the contaminant source was an important factor in controlling deposition fluxes. PAHs bulk deposition was negatively correlated with meteorological parameters (temperature, wind speed, humidity, and precipitation). No significant correlations between soil concentrations and atmospheric deposition were found along this transect. PAHs in soil samples had combined sources of coal, wood and petroleum combustion, while a simple source of coal, wood and grass combustion for bulk deposition. There were significant positive correlation relationship ($p<0.05$) between annual atmospheric bulk deposition and local PAHs emission, with biomass burning as the major contribution to the total emission of PAHs. This transect acts as an important PAHs source rather than being a sink according to the ratio of deposition/emission. Mountain cold trap effect existed in this transect where the altitude was higher than 1000 m. Long-range transport had an impact on the bulk deposition in summer. And this transect was a source to Tibetan only in summer. The forward trajectory analysis showed

* Corresponding author. Tel.: +86 27 67883152, Fax:+ 86 27 87436235. *E-mail addresses:* shihuaqi@cug.edu.cn (Shihua Qi)

37   most air masses did not undergo long-range transport due to the blocking effect of surrounding

38   mountains. Only a few air masses (<10%) arrived at the eastern and northern region of China or

39   farther regions via long-range transport.

40

43

44   **1. Introduction**

45   Polycyclic aromatic hydrocarbons (PAHs) are ubiquitous environmental contaminants that

46   are produced by anthropogenic emissions such as motor vehicles, industrial processes, domestic

47   heating, waste incineration, tobacco smoke and by natural processes such as forest fires and

48   volcanic eruptions (Keshtkar and Ashbaugh, 2007; Shen et al., 2013). PAHs are of great concern

49   due to their widespread occurrence, long-range transport and toxic effects to ecosystem and

50   human health (Wang et al., 2015).

51   Atmospheric deposition is the most important process that removes these chemicals from the

52   atmosphere and are a major PAHs contributor in remote pristine areas(Wang et al., 2010).

53   Atmospheric deposition is a potential important pathway of trace organic pollutants input to the

54   land surface (Pan et al., 2013; Bari et al., 2014). In the wet deposition, PAHs are either dissolved

55   in or rinsed by the rainfall or associated with particles. This process relies on the distribution of

56   the organic matters diffused in vapor phase and particle phase, particle size distribution, and the

57   Henry's law constant. Dry deposition of PAHs, on the other hand, is on accounted of association

58   of PAHs with particles, related to the type of the surface, resistance to mass transfer in the

59   deposition layer (Ollivon et al., 2002; Terzi and Samara, 2005). The total deposition consists of

60   wet and dry deposition. However, it is hard to collect wet and dry deposition separately for

61   long-term sampling especially in remote regions with insufficient electricity supply. Hence, the

62   total deposition can be expressed by the sum of wet and dry deposition, namely "bulk" deposition,

63   which does not discriminate any of the processes and , as a consequence, it sums up all of them

64   (Motelay-Massei et al., 2003; Gocht et al., 2007; Esen et al., 2008; Zhang et al., 2008; Wang et al.,

65   2011). Transport and fate of PAHs in the atmospheric bulk deposition partly depended on their

66   physicochemical characteristics, atmospheric concentration, meteorological condition, topography

67   and emission density (Gocht et al., 2007; Esen et al., 2008; Wang et al., 2011; Zhong and Zhu,

68   2013). Conversely, the atmospheric deposition affected on the equilibrium partitioning of

69   semi-volatile organic chemicals (SOCs) between air and surface, and finally had a strongly

70   influence on the long-term distribution of SOCs in the regional/global environment. So the leading

71   parameter in the process of SOCs transport varies from region to region (Schenker et al., 2014).

72   In western China, steep altitudinal transects separated the highly populated and intensively

73   cultivated Chengdu Plain from the Tibetan Plateau. It is reported as important pathway of some

74   persistent organic pollutants (POPs) from the vicinity of source regions in Chengdu Plain to the

75   Tibetan, which acts as the cold trap of airborne contaminants. Up to date, the majority of reports

76   were focused on OCPs, PCBs, PCNs, PCDD/Fs and PBDEs in soil, atmosphere and biota in this

77   region (Chen et al., 2008; Gong et al., 2010; Liu et al., 2010; Xing et al., 2010; Wang et al., 2012;

78   Liu et al., 2013; Pan et al., 2013; Liu et al., 2014). However, information is limited on the

79   atmospheric deposition contamination by PAHs in in this region. Sichuan Province is one of the

80   most developed provinces in China and the total PAH emission in Sichuan ranked first in China

81   in 2003 with average emission of 5.35 kg km^{-2} (Zhang et al., 2007). Hence, the impact of

82   atmospheric deposition can not be ignored when studying the transport of PAHs and other

83   similar contaminates.

84   This paper presents the result of atmospheric bulk deposition variation in the Chengdu

85   Plain-mountain transect in western China with the aim of clarifying the role of Chengdu Plain as

86   the primary emitter or middle path for POPs to Tibetan Plateau. Specifically, the main aims are:

87   (1) clarifying the temporal and spatial characteristics of atmospheric deposition flux of PAHs; (2)

88   to explore the key factor which affecting PAH deposition; and (3) to distinguish the potential role

89   of this region (acting as a source or sink) according to the trajectory analysis.

90   **2. Experiment and methods**

91   *2.1. Sampling*

92   The study region is located in the centre of Sichuan Province. The geography can be divided

93   into four types: corrosive tectonic mountain of Tibetan Plateau east slope, Longmen Orogenic

94   Piedmont Belt Accumulation Plain, Corrosive Tectonic Hills of east Sichuan Basin and Corrosive

95   Tectonic Mountain of southwest Sichuan Basin. To describe PAHs deposition characteristic in this

96   region, a typical plain-mountain transect was chosen, including low hills in the east, plain in the

97   intergrades and high mountains in the west, which forms part of the eastern slope of Tibetan

98   Plateau (Fig.1), namely "Plain-mountain transect (PMT)". The dominant wind direction (Southern

99   east-northern west) in this region is also along this transect due to the presence of Tibetan in the

100   northern west and monsoon climate in this region.

101   The atmospheric bulk deposition samplers were deployed at ten sites from Daying to

102   Qingping during 16th June 2007 to 27th June 2008 (Fig.1). Detailed site information is listed in

103   Table S1. The sampling programme was conducted for one year of four consecutive seasons

104   (about every three months). The four periods from 16th June to 22nd September, 2007; 22nd

105   September to 24th December, 2007; 24th December, 2007 to 22nd March 2008; and 22nd March

106   2008 to 27th June 2008 were presented as summer, autumn, winter and spring respectively.

107   Bulk deposition (both dry and wet deposition) collection was achieved using a glass funnel

108   with a receiving area of 0.0225m^2, attached to a filter holder which was installed one meter above

109   the ground or on the roof. Fallout was collected in a 4 L brown glass bottle wrapped with

110   aluminium foil to prevent photodegradation. A long ring-shaped silica tube was used to link the

111   funnel and collected bottle to conduct deposition and prevent volatilization. Prior to the filed

112   campaign, the funnels and the bottles were pre-cleaned using acid lotion and rinsed by deionized

113 water, then dried in an oven at 200 °C for 4 hours, and wrapped with aluminium foil. Before

114 set-up, each device was washed and triple rinsed with dichloromethane (DCM). Hydrated copper

115 sulphate ($CuSO_4.\cdot5H_2O$) was added to the bottles to inhibit microbial degradation. The tube was

116 washed with distilled water and DCM, and then wrapped with aluminium foil during transport to

117 the field (Fig.S1). Similar samplers were applied by many researchers (Ollivon et al., 2002;

118 Motelay-Massei et al., 2003; Gocht et al., 2007; Esen et al., 2008; Bari et al., 2014). When we

119 collected the bulk deposition, the surface soil samples were collected as well in the vicinity.

120 Totally, thirty-eight deposition samples and thirty-eight soil samples were collected. Bulk

121 deposition samples at two sites were destroyed during the Earthquake in May 2008. When

122 collecting, the funnels were cleaned with DCM three times and the washings were taken as a part

123 of bulk depositions. After collection, all the samples were preserved in ice boxes and transported

124 to the laboratory as soon as possible and stored at - 20 °C before analysis.
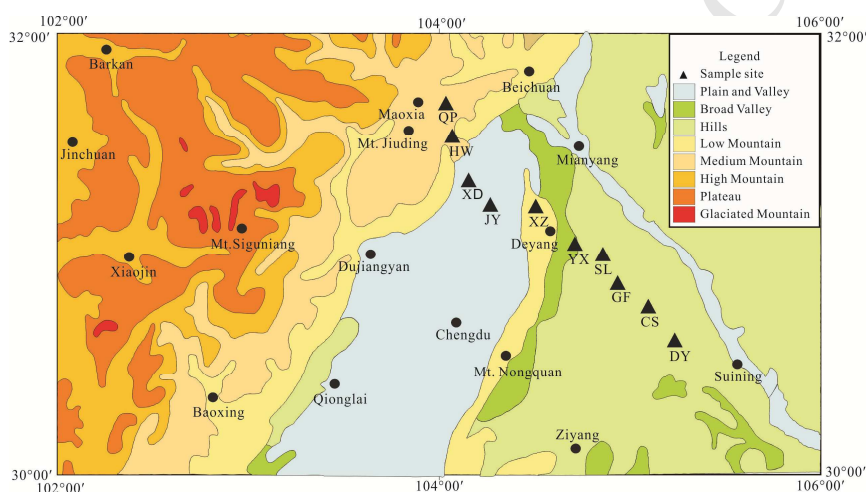
125

126

Fig. 1 Sampling location for atmospheric deposition

127

128 *2.2. Sample extraction and analysis*

129 2.2.1. Extraction

130   The mixture of wet and dry atmospheric deposition samples were defrosted and homogenized

131 by shaking. Then the mixture was separated into the dissolved and particle parts by ultrafiltration

132 with a 0.45μm glass fibre filter membrane. The dissolved one was the water passed through filter

133 membrane and the particles were intercepted by the filter membrane. Both percolator and

134 membrane were cleaned three times by DCM before filtration. The membrane and particle

135 samples were wrapped with aluminium foil. Then particle and water were kept frozen at -20 °C

136 until analysis after about one week.

137   For the particle fraction, the same extraction procedure was followed as soil samples

138 extraction described previously (Xing et al., 2011). Generally, particle were injected with PAH

139 surrogates (naphthalene-d8, acenaphthene-d10, phenanthrene-d10, chrysene-d12 and

140 perylene-d12), and Soxhlet-extracted with dichloromethane (DCM) for 24 h. Small amount of

141 activated copper granules and anhydrous sodium sulphate were added to the extract, then the

4

142 extracts were concentrated and solvent-exchanged to hexane and further reduced to 1-2 mL by a

143 rotary evaporator. A 1:2 (v/v) alumina/silica gel column was used to clean up the extract and

144 targeted compounds were eluted with 30 ml of DCM/hexane (V:V=2:3). The eluate was then

145 concentrated to 0.2 mL under a gentle pure nitrogen stream (purity ⩾ 99.999%).

146 Hexamethylbenzene was added as internal standard prior to instrumental analysis. The filtrated

147 water was extracted using liquid–liquid extraction (LLE) method described in the literatures

148 (Arias et al., 2009; Lohmann et al., 2009; Yang et al., 2013). Briefly, filtrated water was extracted

149 with 40 mL of DCM and 2 g of anhydrous sodium sulphate in a separating funnel and shaken well

150 for 4-5 minutes. The lower DCM layer was collected in a flat bottom flask and the remaining

151 portion was extracted three times with 30 mL of DCM and the extracts were collected in a flat

152 bottom flask. The extracts of water samples were then treated by the same method as particles

153 extracts mentioned above. Finally, 0.2 mL eluate was obtained. Hexamethylbenzene was added as

154 internal standard prior to instrumental analysis.

155 2.2.2. Analysis

156   Sixteen priority control PAHs recommended by the US Environmental Protection Agency

157 were analysed using a GC-MS Agilent 6890N/5975MSD, equipped with a DB-5 capillary column

158 (30 m ×0.25 mm diameter, 0.25 μm film thickness) coupled in the electron impact mode (EI 70 eV,

159 quadrupole temperature 150ºC, ion source temperature 230ºC). The chromatographic conditions

160 were as follows: oven temperature program was initially at 60°C for 5 min and increased to 290°C

161 at a rate of 3°C min^{-1} and kept at 290°C for 40 min, while the temperature for injector and detector

162 was maintained at 270°C and 280°C, respectively. The highly pure (99.999%) carrier gas was

163 helium at a constant flow rate of 1.2 mL min^{-1}. A 1μL concentrated sample was injected with

164 splitless mode. The mass spectrometer was operated in the selected ion monitoring (SIM) mode

165 and tuned with perfluorotributylamine (PFTBA) according to the manufacturer's specifications.

166 Chromatographic peaks of samples were identified by mass spectra and retention time. The PAHs

167 were quantitative analysed according to a 6-point calibration curve of reference materials with

168 internal standard.

169 *2.3. Quality control and quality assurance*

170   Method blanks (solvent), spiked blanks (internal standard compounds spiked into solvent)

171 and field blanks were analysed along with the sample batch. Moreover, 5 μg mL^{-1} PAHs standard

172 solution were was analysed by GC-MSD daily to estimate the method recovery as part of the

173 instrumental quality control. Five PAHs surrogates consisting of naphthalene-D$_{12}$,

174 acenaphthene-D$_{10}$, phenanthrene-D$_{10}$, chrysene-D$_{12}$ and perylene-D$_{12}$ standards were spiked to

175 each sample before extraction. The surrogate recoveries ranged from 70.1%-108.6%. The

176 concentrations of PAHs were corrected by surrogate recoveries.The three times of the

177 signal-to-noise level in the lowest concentration (0.2 μg/mL) standard samples was used as the

178 instrumental detection limit (IDLs). The IDLs of each substance was listed in Table S2. Mass

179 spectrometry was evaluated by mass tuning. The retention times and areas of compounds in spiked

180 blanks were consistent with daily standard sample chromatograms. Calibration curves were was

181 adapted to period check with injection of standard solutions.

182 *2.4. Introductory remarks on the data set*

183   Additional information on flux calculations, meteorological data sources, and a full list of

184 analytes is given in the supporting information Text S1.

185 **3.   Results and discussion**

186 *3.1 General characteristic of annual deposition fluxes*

187   Annual bulk deposition fluxes of PAHs were calculated and summary data are presented in

188 Table 1 and Fig S2. The results showed that total PAHs bulk deposition fluxes ranged from 169.19

189 $\mu g\ m^{-2}\ yr^{-1}$ at XZ to 978.58 $\mu g\ m^{-2}\ yr^{-1}$ at SL, with the geometric mean of 354.22 $\mu g\ m^{-2}\ yr^{-1}$. The

190 proportion of PAH congeners along with the deposition profile was dominated by 3-ring (35.56%)

191 and 4-ring (39.65%) PAHs, followed by 5-6-ring (18.18%) and 2-ring (3.61%) PAHs, with the

192 fluxes of semivolatile PAHs Fla, Phe and Pry were higher than other PAHs on the annual basis.

193   The comparison of deposition fluxes in study area and other regions is listed in Tables S3.

194 The deposition flux in study area was comparable to those previously study in south China, it was

195 higher than that report in more industrialized or urbanized region like Pearl River Delta, China

196 during 2003-2004 ($140\pm89\ \mu g\ m^{-2}\ yr^{-1}$) (Li et al., 2010), but it was slight lower than the report

197 value at Guangzhou during 2001-2002 (mean 460 $\mu g\ m^{-2}\ yr^{-1}$) (Li et al., 2009). The flux was much

198 less than the value in north China, where the deposition flux was $5.22\pm3.89\ \mu g\ m^{-2}\ day^{-1}$ in

199 Beijing-Tianjin region (Wang et al., 2011), 4.88$\mu g\ m^{-2}\ day^{-1}$ in Tianjin and 5.14 $\mu g\ m^{-2}\ day^{-1}$ in the

200 rural of Beijing. Compared with other rural or suburban area in the world, the result was of same

201 order of magnitude as that reported in the rural of southern Germany (73.49-388.01$\mu g\ m^{-2}yr^{-1}$)

202 (Gocht et al., 2007), however it was higher than that in the suburban in the Seine Basin of France

203 (47.85$\mu g\ m^{-2}\ yr^{-1}$) (Motelay-Massei et al., 2003), and that in remote site of northern Spain

204 (60.5$\pm16.4\ \mu g\ m^{-2}yr^{-1}$) (Foan et al., 2015).

205 <div align="center">Table 1 Summary of annual bulk deposition ($\mu g\ m^{-2}\ yr^{-1}$) of selected PAHs</div>

Compounds	Geometric mean	Average ±std	Median	Range
$\sum_{-15}$PAHs	354.22	410.12 ±248.56	358.87	169.19-978.58
Acy	1.45	3.58 ± 4.93	0.93	0.20 -14.37
Ace	0.22	0.25±0.13	0.24	0.08-0.53
Flu	10.80	12.07±5.82	11.76	4.57-23.42
Phe	61.88	71.55±43.33	60.11	30.92-170.69
Ant	7.92	11.15±11.87	6.47	3.60-41.78
Fla	63.35	78.44±58.84	65.87	25.10-219.59
Pyr	43.33	53.24±39.84	45.81	20.98-149.15
BaA	14.34	18.25±14.43	12.73	6.17 -49.81-

Chr	30.18	35.48 ±21.43	29.32	15.49 -74.64-
BbF	29.36	32.34 ±13.67	32.46	12.09 -53.71
BkF	19.73	23.51±15.44	18.38	8.48 -58.29
BaP	12.28	13.42±5.87	13.89	6.28 -23.91
IcdP	24.02	27.22 ±13.76	23.90	9.86 -48.25
DahA	5.39	6.12 ±3.05	5.14	1.93 -10.77
BghiP	21.08	23.48 ±11.46	20.14	11.49 -42.19

206

207 *3.2 Spatial and seasonal variations of atmospheric deposition fluxes*

208   The geographic distribution of PAHs bulk deposition flux in four seasons is shown in Fig.2.
209 In general, higher fluxes of total PAHs were observed in the middle of this transect (DY, SL and
210 JY, the cities and towns around these sites are usually more industrialized or urbanized than in
211 remote sites); lower fluxes were observed at remote areas sites (HW and QP). The deposition
212 fluxes in SL were higher than in the surrounding rural areas sites and even higher than in JY, the
213 urban area site. The Shuanglong petrol station is on the opposite of SL site. Local point emission
214 in SL was an important reason for high deposition flux during sampling period possibly. Due to
215 the different physicochemical properties and sources of PAHs, there were spatial trends of
216 individual compounds. Higher proportion of 4-ring PAHs in higher deposition fluxes sites
217 indicated the 4-ring PAHs were the main contributor to the higher fluxes of bulk deposition.
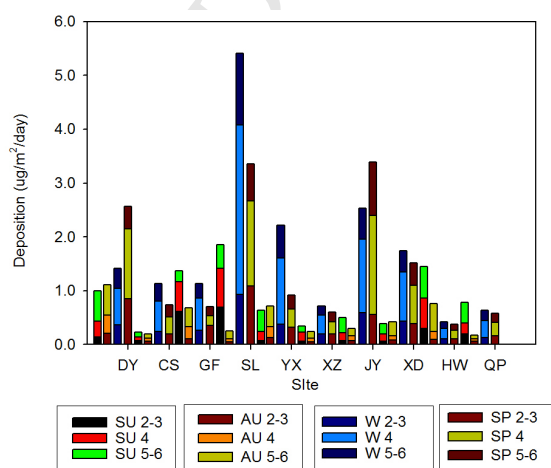
218
219   Fig.2 The seasonal and spatial variation of different rings PAHs bulk deposition
220 (SU means summer samples, AU means autumn samples, W means winter samples and SP means spring samples.
221 And the numbers behind the capital letters mean the number of rings in the PAHs structure.)
222

223   For seasonal variation, the deposition fluxes in cold seasons (winter and spring) were higher
224 than those in warm seasons (summer and autumn). The high fluxes in winter and spring were
225 mainly due to a higher proportion of 4-ring PAHs than the other PAHs. 4-ring PAHs include Fla,
226 Pyr, BaA, and Chr. They are representative of coal combustion and vehicle emission source

7

227   (Khalili et al., 1995; Wang et al., 2008; Gregoris et al., 2014). In the cold seasons, more heating

228   and warming demand will increase the combustion of coal, resulted in high emission of 4-ring

229   PAHs. Meanwhile, the depositions of 4-ring PAHs in cold season were higher than in other

230   seasons, indicating deposition of PAHs was consistent with the emission of PAHs. The seasonality

231   of contaminant source could be an important factor in controlling the deposition fluxes. The result

232   was in accordance with researches in other regions (Li et al., 2010; Wang et al., 2011). Besides the

233   sources emission, the meteorological parameters are also decisive factors for the deposition fluxes.

234   For example, temperature can affect the vapor-particle partitioning for SOCs (Jurado et al., 2004).

235   And the intensity, form (rain or snow) and rate of precipitation, wind speed and humidity could

236   have impacts on the washout ratio and/or dry deposition speed, which will cause the variation of

237   deposition fluxes (Lei and Wania, 2004; Li et al., 2009). It means that the lower temperature and

238   precipitation in the form of snow may have a higher scavenging ratio of PAHs in atmosphere.

239   Moreover, the forest canopies can deplete of gaseous PAHs (Choi et al., 2008). Seasonal changes

240   of forest canopies can affect the concentration of more volatile PAHs in the atmosphere. Thus the

241   fluxes of PAHs with less rings in warm seasons was lower than those in the cold seasons.

242   Comprehensively, all the above factors may result the seasonal varying of PAHs deposition fluxes.

243   To clarify this issue in this junction between Chengdu Plain and east edge of Tibetan, the variation

244   controlling factors of deposition fluxed are discussed below according to the collected data.

245   *3.3 Controlling factors for the atmospheric bulk deposition fluxes*

246   3.3.1 The influence of meteorological parameters on deposition fluxes

247   Meteorological conditions can affect PAHs in term of their generation, phase partition,

248   diffusion, removal, etc.(He et al., 2014). The typical subtropical monsoon climate in Guangzhou

249   played a key role in controlling seasonal variation of PAHs concentration and particle deposition

250   fluxes (Li et al., 2010). High ambient temperature are correlated with low deposition rates in rural

251   area of southern Germany (Gocht et al., 2007). The relationship between PAHs atmospheric bulk

252   deposition and meteorological factors was analysed using IBM SPSS Statistics 20 and the

253   Spearman correlation coefficients are shown in Table S4. Generally, negative relationship was

254   found in mean of daily deposition bulk in every season versus temperature, wind speed, humidity,

255   and precipitation for 4-rings and 2-3 rings PAH compounds. The deposition fluxes of 2-3 ring and

256   4-ring PAHs were much higher than those of 5-6 ring PAHs (Fig.2). Hence, we can conclude

257   PAHs bulk deposition was negatively correlated to those meteorological parameters. Similar

258   results were reported in fine particulate matter in Nanjing, China (He et al., 2014) and particle

259   deposition fluxes in Guangzhou (Li et al., 2010). However, for other POPs (e.g. pesticide such as

260   HCHs and HCBs), stronger temperature dependencies were observed for high atmospheric

261   concentration during warming periods and lower ones in the cold periods (Gioia et al., 2005). The

262   possible reason was thermodynamically derived distribution (via evaporation from nearby

263   terrestrial surfaces or long-range transport) for those compounds and primary emission density

264   controlling patterns for PAHs in this study area.

265

266   3.3.2 The relationship between local emission and atmospheric deposition fluxes

267   As PAHs production is associated with anthropogenic activities such as domestic and

268   industrial heating, traffic petrol combustion, the population density as well, so the local emission

269   may explain the variations of PAHs deposition fluxes.

270   Local emission data was obtained from global atmospheric emission data of PAHs (Shen et

271   al., 2013) http://inventory.pku.edu.cn/data/data.html. The data we used was the annual average

272   value of the year 2007-2008 to match our sampling period. In the Fig.3, the total 15 PAHs bulk

273   deposition profile showed well coincides with the total local emission (2007-2008) in most

274   sampling site except for Site XD. As PAHs is associated with human activities, local emission can

275   be reflected on atmospheric bulk deposition fluxes. This transect is not only a pathway for PAHs

276   transport, but also an important source at low altitude region (except remote mountain site QP).
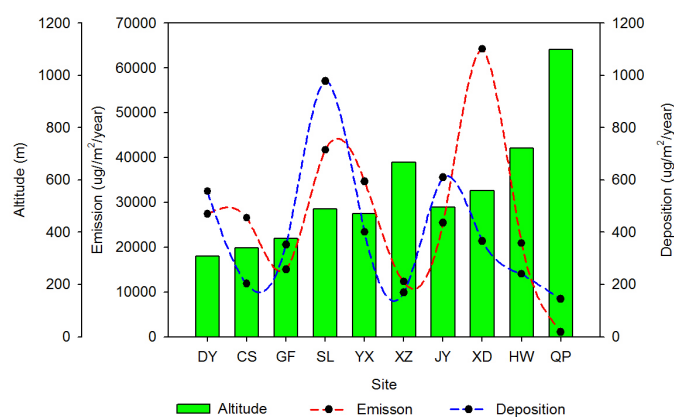

277

278   Fig.3$\sum_{15}$-PAHs bulk deposition vs. total local emission

279

280   In Fig. 4, the logarithm of the category of PAHs emission vs. bulk deposition was

281   demonstrated. The detailed information on every category was obtained from

282   http://inventory.pku.edu.cn/data/data.html (Shen et al., 2013), and the description of every

283   category can be found in the supporting information (Table S5). In Fig. 4, biomass combustion

284   presented the main contribution to the local emission of PAHs, secondly was coal, and then

285   followed by process, oil, waster, gas and open fire. There were obvious positive correlation

286   (p<0.05) between annual atmospheric bulk deposition and PAHs emission, especially with

287   biomass, oil and waste combustion (Table S6), which confirmed human activity affected the

288   deposition fluxes of PAHs. In addition, principal component analysis (PCA) was applied to

289   confirm the diagnostic testing. Total variability of the original data (depositions, biomass, coal, gas,

290   oil, process and waste) was represented during the PCA (Fig. S3). The first two principal

291   components (PCs), with eigenvalues greater than 1, accounted for 90.26% of the total variance in

292   the data set. As shown in Fig. S3, PC1, which explained 63.78% of the total variance, was highly

293   dominated by coal, gas, oil and process. It also had a large loading for biomass and waste. The

294   angles between deposition and the six emissions were all acute angles, indicating a positive

9

295 correlation between deposition and those emissions. PC2 accounted for 26.48% of the total

296 variance and was heavily weighted by deposition. PC2 had a high negative loading of open fire,

297 indicating no significant correlation of open fire with deposition.
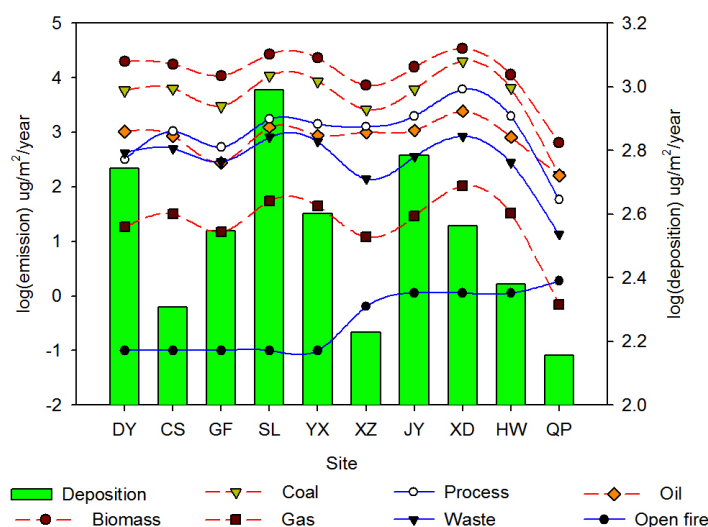
298

299 Fig.4 $\sum_{15}$-PAHs bulk deposition vs. different category emission in the form of logarithm

300 (For site DY, CS, GF, SL and YX, there was no open fire emission, for the transform of logarithm, -1 was given to

301 those values)

302

303 The emission fluxes of PAHs were hundreds of times higher than the deposition fluxes,

304 which indicated much more PAHs were preferentially transported to other area than to deposit in

305 local area, and thus this area was an important source region during the transport of PAHs. To

306 determine the role of this transect (source or sink), the relationship between deposition and

307 emission, the budget of deposition and emission were calculated. Firstly, the hypothesis deposition

308 from local emission totally was given. The deposition efficiency was calculated according to the

309 deposition divided by emission. In Fig.S4, the influence of altitude and molecular weight of PAHs

310 on the efficiency of deposition is shown. There was no obvious difference for site below 1000 m

311 a.s.l.. As the altitude increased more than 1000 m, the ratio of deposition/emission increased. One

312 possible reason was that the emission at region with higher altitude was less than that in Chengdu

313 Plain (Shen et al., 2013); another reason was mountain had a cold trap for POPs, especially for

314 heavy molecular weight compounds (Chen et al., 2008). 5-6 ring PAHs had higher

315 deposition/emission value than 2-3 and 4 ring PAHs. As rings of PAHs increased, the efficiency of

316 deposition was enhanced, which also suggested the light molecular PAHs had higher potentiality

317 to undergo long-range transport.

318 *3.4 Effect of deposition on soil burdens*

319 Soil plays an important role in the transport of POPs. It always acts as the sink during the

320 orographic cold trapping as altitude increases due to high precipitation rates and organic carbon

321 content (Daly and Wania, 2005; Daly et al., 2007; Chen et al., 2008; Choi et al., 2009; Sheng et al.,

322 2013), and simultaneously soil played the role of source for volatile compounds evaporation to

323 atmosphere when the equilibrium was broken between soil and air exchange (Cabrerizo et al.,

324   2011; Qu et al., 2015). The relationship between atmospheric deposition flux and soil

325   concentration is shown in Fig.5. Generally, soil concentrations in most sites increased with altitude

326   along this transect, and displayed maxima at intermediate elevations at XZ, a suburban site near

327   Chengdu. These distribution patterns can be understood as being determined by the balance

328   between atmospheric depositions and retention within the soils. However, for deposition flux,

329   there was no significant increase. Neither significant correlations between soil concentrations and

330   atmospheric deposition were observed along this transect. It also confirmed our conclusion that no

331   thermodynamically distribution dominated in this region. The variation of PAHs concentration in

332   soil was less than atmospheric deposition during different seasonal sampling, which possibly

333   indicated soil was more stable than atmospheric deposition to the changes of PAHs emission, and

334   thus explained why no positive relationship was found here for soil concentration and atmospheric
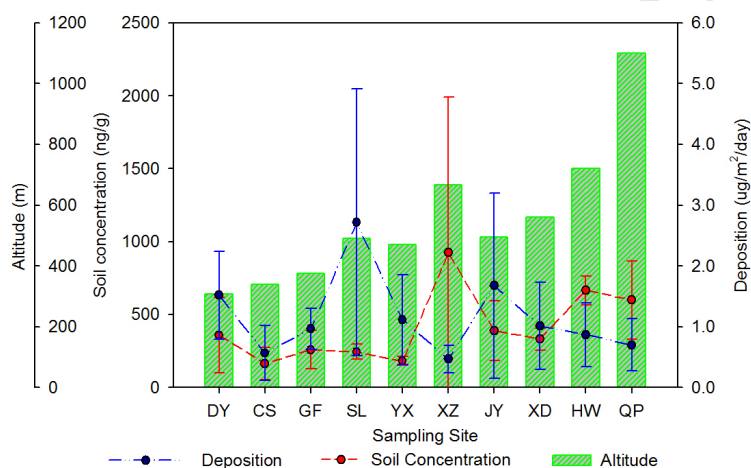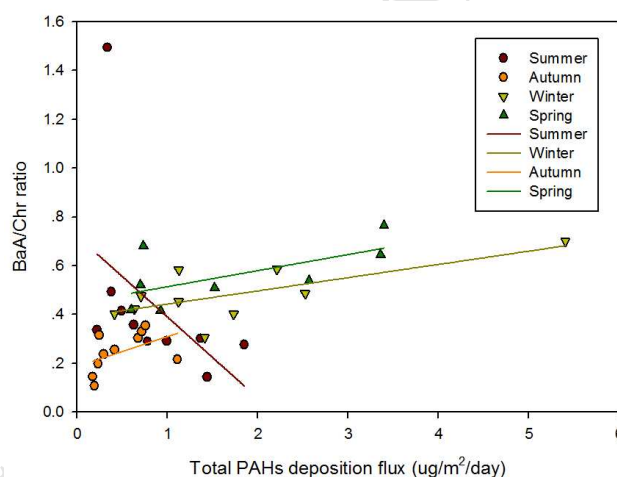
335   deposition.

336

337   Fig. 5 Soil concentrations vs. atmospheric bulk deposition flux in sampling sites of different altitudes

338

339   The molecular indices IcdP/(IcdP + BghiP) and Flu/(Flu + Pyr) were used to distinguish the

340   PAHs source for soil and atmospheric deposition in this study according to study in other regions

341   (Ding et al., 2007; Xing et al., 2011; Gregoris et al., 2014; Bosch et al., 2015; Chen et al., 2015;

342   Hong et al., 2015; Ma and Harrad, 2015; Zhang et al., 2015). The data for the ratios of these

343   compounds in the atmospheric deposition and soil samples are presented in Fig.S5. The IcdP/(IcdP

344   + BghiP) values for most samples were >0.5, suggesting that coal and wood combustion may be

345   the predominant source of PAHs in atmospheric deposition, while PAHs ratios in soils were

346   mainly between 0.3-0.7, indicating a more complicated PAHs sources derived from mixed

347   combustion of coal wood and petroleum combustion. The ratios of Fla/(Fla + Pry) from

348   atmospheric deposition showed PAHs mainly derived from combustion of coal, wood and grass as

349   well. However, PAHs in soil arise from a complex mixture of sources, including both biomass

350   combustion as well as fossil fuel combustion, which fits well with the result from IcdP/(IcdP +

351   BghiP). According to biplots of IcdP/(IcdP + BghiP) versus Fla/(Fla + Pry) ratio for soil and

352   atmospheric deposition, the results suggested combustion of coal, grass and wood was major

11

353   source of PAHs in atmospheric deposition, while soil arose from a complex mixture of sources,

354   including both combustion for rooms heating and cooking, as well as outdoor emissions from

355   traffic and fossil fuel combustion. This result confirmed why no positive relationship was shown

356   for soil and atmospheric deposition.

357   *3.5 Influence of regional atmospheric transport of PAHs on deposition fluxes*

358   Air mass transport can bring in pollutants from distance areas, thus affecting local PAHs

359   concentration in atmosphere. It was reported that the impact of local or regional transport can be

360   reflected by the ratio of more reactive PAHs to a stable PAH, such as the ratio of BaA/Chr can be

361   employed to illustrate whether the collected air masses are fresh or aged. A higher ratio indicates

362   relatively little photochemical processing of the air mass and major impact from local emissions.

363   On the other hand, a lower ratio is reflective of more aged PAHs (Ding et al., 2007). Fig. 6

364   revealed the relationship between BaA/Chr and PAHs deposition fluxes in different seasons.

365   Generally, a slight positive relationship was shown during the periods of autumn, winter and

366   spring, as PAHs deposition increased, the ratios of BaA/Chr become higher, indicating the

367   elevated deposition was mainly contribution of local emission. While in summer sampling periods,

368   a negative relationship was presented, illuminating long-range transport had a higher impact on

369   the deposition in summer.

370

371   Fig.6 The relationship between BaA/Chr and PAHs deposition fluxes

372

373   In order to identify potential source regions and transport pathways, 5-day backward and

374   foreword trajectories arriving at 100 meters above ground level for one year between June 2007

375   and June 2008 at the sampling site were generated using the PC Version HYSPLIT 4 model

376   (http://www.arl.noaa.gov/ready/hysplit4.html) respectively. This model was developed by

377   NOAA/ARL (US National Oceanic and Atmospheric Administration/Air Resources Laboratory).

378   The seasonal trajectories after cluster are presented in Fig.S6 and Fig.S7.

379   The back trajectory maps are shown in Fig.S6, which indicated local emissions were the

380   dominant source (more than 40 % of total air mass) for PAHs deposition in the study area during

381   sampling time. Second source was the eastern and northern part of China. The air mass from the

countries west to China such as Indian and Nepal, which underwent long-rang transport also arrived in this region. In summer, during the summer monsoon period, a high percentage contribution (21% of air masses) from the south of China entered the study area as well. It confirmed our conclusion that the long-range transport has a higher impact on the atmospheric deposition during summer. The annual back trajectory map showed the same result as the seasonal conclusions. Most air masses were originated from local or nearby regions (36%). Due to the influence of eastern monsoon, the high contribution (28%) was from eastern region as well, followed by air mass from the north of China (23%). The air mass from west direction underwent long distance transport, and had small contribution (7% and 6%) to the total air mass in the study region. It indicated the spatial variation in bulk deposition was mainly effected by the local emission in our study.   As mentioned above, only a little local emission PAHs was loaded in situ, most PAHs may undergo long-rang transport to other region. The study in Wolong near our study area reported air mass from lower altitude Chengdu might enter western mountains (Pan et al., 2013). The forward trajectory maps (Fig.S7) show the possible sink/fate of pollutants originated from our study area. In summer, about 10% of air masses originating from the Chengdu Plain indeed entered the western part of China, e.g. the Tibet. However, most air masses did not undergo long-range transport. The mountains surrounding Chengdu Plain blocked them. Only a small fraction of air masses (<10%) which underwent long-range transport, the main destinations were the eastern and northern regions of China or farther regions.

4.   Conclusions

The bulk deposition fluxes of $\sum_{15}$-PAHs ranged from 169.19 μg m^{-2} yr^{-1} to 978.58 μg m^{-2} yr^{-1}, with the geometric mean of 354.22 μg m^{-2} yr^{-1} along a plain–mountain transect in Chengdu Plain, West China, from Daying to Qingping. Higher fluxes of total PAHs were observed in the middle of this transect (urbanized sites, SL, YX and JY). The deposition fluxes of $\sum_{15}$-PAHs in cold seasons (winter and spring) were higher than those in warm seasons (summer and autumn), indicating that the seasonal variation of contaminant source was an important factor in controlling the deposition fluxes.

PAHs bulk deposition was negatively correlated with meteorological parameters (temperature, wind speed, humidity and precipitation). No significant correlations were found between soil concentrations and atmospheric deposition along this transect. The biplots of IcdP/(IcdP + BghiP) vs. Fla/(Fla + Pry) indicated a more complex source for soil while simple combustion source of coal, wood and grass for bulk deposition was shown. There were obvious positive correlation (p<0.05) between annual atmospheric bulk deposition and PAHs emission, and biomass was the main contributor to the total emission of PAHs.

According to the ratio of deposition/emission, this transect played an important role as a source of PAHs rather than a sink. Mountain cold trap existed in this transect where altitude was

419 higher than 1000 meters. The ratio of BaA/Chr and back trajectory indicated that high atmospheric

420 deposition was closely associated with local emission. While long-range transport had an

421 important impact on the deposition fluxes in summer. The forward trajectory illuminated this

422 transect was a source to Tibet only in summer. Most air mass in this study did not undergo

423 long-range transport due to the blocking effect of surrounding mountains. Only a few air masses

424 (<10%) underwent long-range transport to the eastern and northern regions of China or farther

425 regions.

426

433

434 **References**

435 Arias, A.H., Spetter, C.V., Freije, R.H., Marcovecchio, J.E., 2009. Polycyclic aromatic hydrocarbons in

436 water, mussels (Brachidontes sp., Tagelus sp.) and fish (Odontesthes sp.) from Bahía Blanca Estuary,

437 Argentina. Estuarine, Coastal and Shelf Science 85, 67-81.

438 Bari, M.A., Kindzierski, W.B., Cho, S., 2014. A wintertime investigation of atmospheric deposition of

439 metals and polycyclic aromatic hydrocarbons in the Athabasca Oil Sands Region, Canada. Science of

440 the Total Environment 485, 180-192.

441 Bosch, C., Andersson, A., Krusa, M., Bandh, C., Hovorkova, I., Klanova, J., Knowles, T.D.J., Pancost,

442 R.D., Evershed, R.P., Gustafsson, O., 2015. Source Apportionment of Polycyclic Aromatic

443 Hydrocarbons in Central European Soils with Compound-Specific Triple Isotopes (delta C-13, Delta

444 C-14, and delta H-2). Environmental Science & Technology 49, 7657-7665.

445 Cabrerizo, A., Dachs, J., Jones, K.C., Barcelo, D., 2011. Soil-Air exchange controls on background

446 atmospheric concentrations of organochlorine pesticides. Atmospheric Chemistry and Physics 11,

447 12799-12811.

448 Chen, D., Liu, W., Liu, X., Westgate, J.N., Wania, F., 2008. Cold-trapping of persistent organic

449 pollutants in the mountain soils of Western Sichuan, China. Environmental Science & Technology 42,

450 9086-9091.

451 Chen, P.F., Kang, S.C., Li, C.L., Rupakheti, M., Yan, F.P., Li, Q.L., Ji, Z.M., Zhang, Q.G., Luo, W.,

452 Sillanpaa, M., 2015. Characteristics and sources of polycyclic aromatic hydrocarbons in atmospheric

453 aerosols in the Kathmandu Valley, Nepal. Science of the Total Environment 538, 86-92.

454 Choi, S.-D., Shunthirasingham, C., Daly, G.L., Xiao, H., Lei, Y.D., Wania, F., 2009. Levels of

455 polycyclic aromatic hydrocarbons in Canadian mountain air and soil are controlled by proximity to

456 roads. Environmental Pollution 157, 3199-3206.

457 Choi, S.D., Staebler, R.M., Li, H., Su, Y., Gevao, B., Harner, T., Wania, F., 2008. Depletion of gaseous

458   polycyclic aromatic hydrocarbons by a forest canopy. Atmospheric Chemistry and Physics 8,

459   4105-4113.

460   Daly, G.L., Lei, Y.D., Teixeira, C., Muir, D.C.G., Wania, F., 2007. Pesticides in western Canadian

461   mountain air and soil. Environmental Science & Technology 41, 6020-6025.

462   Daly, G.L., Wania, F., 2005. Organic contaminants in mountains. Environmental Science & Technology

463   39, 385-398.

464   Ding, X., Wang, X.-M., Xie, Z.-Q., Xiang, C.-H., Mai, B.-X., Sun, L.-G., Zheng, M., Sheng, G.-Y., Fu,

465   J.-M., Pöschl, U., 2007. Atmospheric polycyclic aromatic hydrocarbons observed over the North

466   Pacific Ocean and the Arctic area: Spatial distribution and source identification. Atmospheric

467   Environment 41, 2061-2072.

468   Esen, F., Cindoruk, S.S., Tasdemir, Y., 2008. Bulk deposition of polycyclic aromatic hydrocarbons

469   (PAHs) in an industrial site of Turkey. Environmental Pollution 152, 461-467.

470   Foan, L., Domercq, M., Bermejo, R., Miguel Santamaria, J., Simon, V., 2015. Mosses as an integrating

471   tool for monitoring PAH atmospheric deposition: Comparison with total deposition and evaluation of

472   bioconcentration factors. A year-long case-study. Chemosphere 119, 452-458.

473   Gioia, R., Offenberg, J.H., Gigliotti, C.L., Totten, L.A., Du, S., Eisenreich, S.J., 2005. Atmospheric

474   concentrations and deposition of organochlorine pesticides in the US Mid-Atlantic region. Atmospheric

475   Environment 39, 2309-2322.

476   Gocht, T., Klemm, O., Grathwohl, P., 2007. Long-term atmospheric bulk deposition of polycyclic

477   aromatic hydrocarbons (PAHs) in rural areas of Southern Germany. Atmospheric Environment 41,

478   1315-1327.

479   Gong, P., Wang, X., Sheng, J., Yao, T., 2010. Variations of organochlorine pesticides and

480   polychlorinated biphenyls in atmosphere of the Tibetan Plateau: Role of the monsoon system.

481   Atmospheric Environment 44, 2518-2523.

482   Gregoris, E., Argiriadis, E., Vecchiato, M., Zambon, S., De Pieri, S., Donateo, A., Contini, D., Piazza,

483   R., Barbante, C., Gambaro, A., 2014. Gas-particle distributions, sources and health effects of polycyclic

484   aromatic hydrocarbons (PAHs), polychlorinated biphenyls (PCBs) and polychlorinated naphthalenes

485   (PCNs) in Venice aerosols. Science of the Total Environment 476–477, 393-405.

486   He, J., Fan, S., Meng, Q., Sun, Y., Zhang, J., Zu, F., 2014. Polycyclic aromatic hydrocarbons (PAHs)

487   associated with fine particulate matters in Nanjing, China: Distributions, sources and meteorological

488   influences. Atmospheric Environment 89, 207-215.

489   Hong, Y.W., Chen, J.S., Zhang, F.W., Zhang, H., Xu, L.L., Yin, L.Q., Chen, Y.T., 2015. Effects of

490   urbanization on gaseous and particulate polycyclic aromatic hydrocarbons and polychlorinated

491   biphenyls in a coastal city, China: levels, sources, and health risks. Environmental Science and

492   Pollution Research 22, 14919-14931.

493   Jurado, E., Jaward, F.M., Lohmann, R., Jones, K.C., Simo, R., Dachs, J., 2004. Atmospheric dry

494   deposition of persistent organic pollutants to the Atlantic and inferences for the global oceans.

495   Environmental Science & Technology 38, 5505-5513.

496   Keshtkar, H., Ashbaugh, L.L., 2007. Size distribution of polycyclic aromatic hydrocarbon particulate

497   emission factors from agricultural burning. Atmospheric Environment 41, 2729-2739.

498   Lei, Y.D., Wania, F., 2004. Is rain or snow a more efficient scavenger of organic chemicals?
499   Atmospheric Environment 38, 3557-3571.

500   Li, J., Cheng, H., Zhang, G., Qi, S., Li, X., 2009. Polycyclic aromatic hydrocarbon (PAH) deposition to
501   and exchange at the air-water interface of Luhu, an urban lake in Guangzhou, China. Environmental
502   Pollution 157, 273-279.

503   Li, J., Liu, X., Zhang, G., Li, X.-D., 2010. Particle deposition fluxes of BDE-209, PAHs, DDTs and
504   chlordane in the Pearl River Delta, South China. Science of the Total Environment 408, 3664-3670.

505   Liu, H., Qi, S., Yang, D., Hu, Y., Li, F., Liu, J., Xing, X., 2013. Soil concentrations and soil-air
506   exchange of organochlorine pesticides along the Aba profile, east of the Tibetan Plateau, western China.
507   Frontiers of Earth Science 7, 395-405.

508   Liu, W., Chen, D., Liu, X., Zheng, X., Yang, W., Westgate, J.N., Wania, F., 2010. Transport of
509   semivolatile organic compounds to the Tibetan Plateau: spatial and temporal variation in air
510   concentrations in mountainous Western Sichuan, China. Environmental Science & Technology 44,
511   1559-1565.

512   Liu, X., Li, J., Zheng, Q., Bing, H., Zhang, R., Wang, Y., Luo, C., Liu, X., Wu, Y., Pan, S., Zhang, G.,
513   2014. Forest Filter Effect versus Cold Trapping Effect on the Altitudinal Distribution of PCBs: A Case
514   Study of Mt. Gongga, Eastern Tibetan Plateau. Environmental Science & Technology 48, 14377-14385.

515   Lohmann, R., Gioia, R., Jones, K.C., Nizzetto, L., Temme, C., Xie, Z., Schulz-Bull, D., Hand, I.,
516   Morgan, E., Jantunen, L., 2009. Organochlorine pesticides and PAHs in the surface water and
517   atmosphere of the North Atlantic and Arctic Ocean. Environmental Science & Technology 43,
518   5633-5639.

519   Ma, Y.N., Harrad, S., 2015. Spatiotemporal analysis and human exposure assessment on polycyclic
520   aromatic hydrocarbons in indoor air, settled house dust, and diet: A review. Environment International
521   84, 7-16.

522   Motelay-Massei, A., Ollivon, D., Garban, B., Chevreuil, M., 2003. Polycyclic aromatic hydrocarbons
523   in bulk deposition at a suburban site: assessment by principal component analysis of the influence of
524   meteorological parameters. Atmospheric Environment 37, 3135-3146.

525   Ollivon, D., Blanchoud, H., Motelay-Massei, A., Garban, B., 2002. Atmospheric deposition of PAHs to
526   an urban site, Paris, France. Atmospheric Environment 36, 2891-2900.

527   Pan, J., Yang, Y., Zhu, X., Yeung, L.W.Y., Taniyasu, S., Miyake, Y., Falandysz, J., Yamashita, N., 2013.
528   Altitudinal distributions of PCDD/Fs, dioxin-like PCBs and PCNs in soil and yak samples from
529   Wolong high mountain area, eastern Tibet-Qinghai Plateau, China. Science of the Total Environment
530   444, 102-109.

531   Qu, C., Qi, S., Yang, D., Huang, H., Zhang, J., Chen, W., Yohannes, H.K., Sandy, E.H., Yang, J., Xing,
532   X., 2015. Risk assessment and influence factors of organochlorine pesticides (OCPs) in agricultural
533   soils of the hill region: A case study from Ningde, southeast China. Journal of Geochemical
534   Exploration 149, 43-51.

535   Schenker, S., Scheringer, M., Hungerbühler, K., 2014. Do persistent organic pollutants reach a
536   thermodynamic equilibrium in the global environment? Environmental Science & Technology 48,
537   5017-5024.

538 Shen, H.Z., Huang, Y., Wang, R., Zhu, D., Li, W., Shen, G.F., Wang, B., Zhang, Y.Y., Chen, Y.C., Lu, Y.,

539 Chen, H., Li, T.C., Sun, K., Li, B.G., Liu, W.X., Liu, J.F., Tao, S., 2013. Global Atmospheric Emissions

540 of Polycyclic Aromatic Hydrocarbons from 1960 to 2008 and Future Predictions. Environmental

541 Science & Technology 47, 6415-6424.

542 Sheng, J.J., Wang, X.P., Gong, P., Joswiak, D.R., Tian, L.D., Yao, T.D., Jones, K.C., 2013.

543 Monsoon-Driven Transport of Organochlorine Pesticides and Polychlorinated Biphenyls to the Tibetan

544 Plateau: Three Year Atmospheric Monitoring Study. Environmental Science & Technology 47,

545 3199-3208.

546 Terzi, E., Samara, C., 2005. Dry deposition of polycyclic aromatic hydrocarbons in urban and rural

547 sites of Western Greece. Atmospheric Environment 39, 6261-6270.

548 Wang, C.h., Wu, S.h., Zhou, S.l., Wang, H., Li, B.j., Chen, H., Yu, Y.n., Shi, Y.x., 2015. Polycyclic

549 aromatic hydrocarbons in soils from urban to rural areas in Nanjing: Concentration, source, spatial

550 distribution, and potential human health risk. Science of the Total Environment 527, 375-383.

551 Wang, R., Tao, S., Wang, B., Yang, Y., Lang, C., Zhang, Y., Hu, J., Ma, J., Hung, H., 2010. Sources and

552 Pathways of Polycyclic Aromatic Hydrocarbons Transported to Alert, the Canadian High Arctic.

553 Environmental Science & Technology 44, 1017-1022.

554 Wang, W., Simonich, S.L.M., Giri, B., Xue, M., Zhao, J., Chen, S., Shen, H., Shen, G., Wang, R., Cao,

555 J., Tao, S., 2011. Spatial distribution and seasonal variation of atmospheric bulk deposition of

556 polycyclic aromatic hydrocarbons in Beijing-Tianjin region, North China. Environmental Pollution 159,

557 287-293.

558 Wang, X.-p., Sheng, J.-j., Gong, P., Xue, Y.-g., Yao, T.-d., Jones, K.C., 2012. Persistent organic

559 pollutants in the Tibetan surface soil: Spatial distribution, air-soil exchange and implications for global

560 cycling. Environmental Pollution 170, 145-151.

561 Xing, X.L., Qi, S.H., Zhang, J.Q., Wu, C.X., Zhang, Y., Yang, D., Odhiambo, J.O., 2011. Spatial

562 distribution and source diagnosis of polycyclic aromatic hydrocarbons in soils from Chengdu

563 Economic Region, Sichuan Province, western China. Journal of Geochemical Exploration 110,

564 146-154.

565 Xing, X.L., Qi, S.H., Zhang, Y.A., Yang, D., Odhiambo, J.O., 2010. Organochlorine Pesticides (OCPs)

566 in Soils Along the Eastern Slope of the Tibetan Plateau. Pedosphere 20, 607-615.

567 Yang, D., Qi, S., Zhang, Y., Xing, X., Liu, H., Qu, C., Liu, J., Li, F., 2013. Levels, sources and potential

568 risks of polycyclic aromatic hydrocarbons (PAHs) in multimedia environment along the Jinjiang River

569 mainstream to Quanzhou Bay, China. Marine Pollution Bulletin 76, 298-306.

570 Zhang, G., Chakraborty, P., Li, J., Sampathkumar, P., Balasubramanian, T., Kathiresan, K., Takahashi,

571 S., Subramanian, A., Tanabe, S., Jones, K.C., 2008. Passive Atmospheric Sampling of Organochlorine

572 Pesticides, Polychlorinated Biphenyls, and Polybrominated Diphenyl Ethers in Urban, Rural, and

573 Wetland Sites along the Coastal Length of India. Environmental Science & Technology 42, 8218-8223.

574 Zhang, Y., Yu, H.J., Xi, B.D., Hou, H.B., Gao, R.T., Liang, Q., Zhang, H., Xu, F.X., 2015. Levels,

575 sources, and potential ecological risks of polycyclic aromatic hydrocarbons (PAHs) in a typical

576 effluent-receiving river (Wangyang River), North China. Arabian Journal of Geosciences 8, 6535-6543.

577 Zhang, Y.X., Tao, S., Cao, J., Coveney, R.M., 2007. Emission of polycyclic aromatic hydrocarbons in

578   China by county. Environmental Science & Technology 41, 683-687.

579   Zhong, Y., Zhu, L., 2013. Distribution, input pathway and soil-air exchange of polycyclic aromatic

580   hydrocarbons in Banshan Industry Park, China. Science of the Total Environment 444, 177-182.

581

582

Highlights:

➢ Spatio-temporal variations of PAHs in atmospheric deposition were observed.

➢ PAHs deposition was negatively correlated to some meteorological parameters.

➢ Atmospheric PAHs deposition was closely related to local emission.

➢ This transect played an important role of source rather than sink.

➢ Most air mass did not undergo long-range transport due to the presence of mountains.